Electronic Raman scattering of Co^{2+} in $CdCl_2$ and $CsMgCl_3$

J. E. Kardontchik
Department of Physics, Technion, Haifa, Israel

E. Cohen*
Bell Laboratories, Murray Hill, New Jersey 07974

J. Makovsky
Nuclear Research Center, Negev, P.O. Box 9001, Beer Sheva, Israel
(Received 6 May 1975)

The polarized Raman scattering between the electronic levels of the $^4T_{1g}$ ground term of Co^{2+} in $CsMgCl_3$ has been observed at 2°K. We calculated the fine structure of $^4T_{1g}$ for this system as well as for Co^{2+} in $CdCl_2$ (observed by Lockwood and Christie). Second-order perturbation theory has been employed for a Hamiltonian containing the trigonal crystal field Δ and spin-orbit interaction λ. The data are fit satisfactorily with $\Delta/|\lambda| = +4.4$ and -2.5, respectively. Using the crystal-field wave functions we calculated the spectral intensities of the electronic Raman lines as a function of $\Delta/|\lambda|$, within the framework of Axe's theory. The theory predicts a small asymmetry between xz and zx polarizations and a very weak scattering in zz polarization. These predictions result mainly from the fact that the intermediate configuration $3d^6 4p$ lies more than 100000 cm^{-1} above the $3d^7$ configuration, making the closure assumption an adequate approximation. Good agreement is obtained between observed and calculated spectral intensities for both crystals.

I. INTRODUCTION

The electronic Raman scattering by crystals containing transition-metal ions has been used mainly in the study of magnetically ordered systems.[1] This scattering involves the creation of either one or two magnons. Scattering by isolated ions (diluted crystals) was studied in fewer cases[2,3] and the theoretical understanding of this phenomenon has not been thoroughly pursued. By contrast, in the case of crystals containing rare-earth ions the electronic Raman scattering is better understood.[4]

In this work we present experimental results of scattering by Co^{2+} ions imbedded in two crystals: $CdCl_2$ and $CsMgCl_3$. In the latter case a full polarization analysis of the scattering has been obtained. We then develop the theory of the electronic Raman scattering along similar lines used in the case of rare-earth ions (Axe's theory[5]). The scattering intensities are calculated as a function of the parameters which determine the fine structure of the ground term ($^4T_{1g}$): the spin-orbit interaction and the trigonal crystal field. We show that the basic closure approximations involved in the theory hold better for transition-metal ions than for rare earths. This results in good agreement between the theoretically calculated spectral intensities and those observed experimentally.

The paper is outlined as follows: Section II sums up the experimental results; Sec. III deals with fitting the energy levels of the $^4T_{1g}$ term and obtaining the crystalline wave functions. In Sec. IV we present the theory of the electronic Raman scattering and apply it to the $^4T_{1g}$ term.

II. CRYSTAL STRUCTURE AND EXPERIMENTAL RESULTS

Co^{2+} ions occupy sites of D_{3d} symmetry in both $CdCl_2$ and $CsMgCl_3$. (Both crystals are uniaxial, with space groups D_{3d}^5 and D_{6h}^4, respectively.) The electronic Raman scattering of $CdCl_2$: 3-at.% Co^{2+} has been investigated by Lockwood and Christie.[3] They did not obtain a polarization analysis of the spectrum. (It is extremely difficult to cut and polish single crystals of $CdCl_2$ in a plane containing the c axis.) However, the incident light in their experiment traveled perpendicular to the c axis and the scattered light was observed parallel to the c axis. Therefore, the three reported electronic lines were observed in a combination of yx and zx polarizations. (The z direction is chosen parallel to the c axis.)

We have carried out a detailed polarization analysis of the electronic Raman scattering of single crystals of $CsMgCl_3$: 7-at.% Co^{2+}. The crystals were grown by the Bridgman technique.[6] The scattering was observed at 2 °K using the 4880-Å line of an Ar^+ laser and the 6471-Å line of a Kr^+ laser. However, all the analysis was carried out on spectra observed with the latter. This is because the absorption of the Co^{2+} ion in

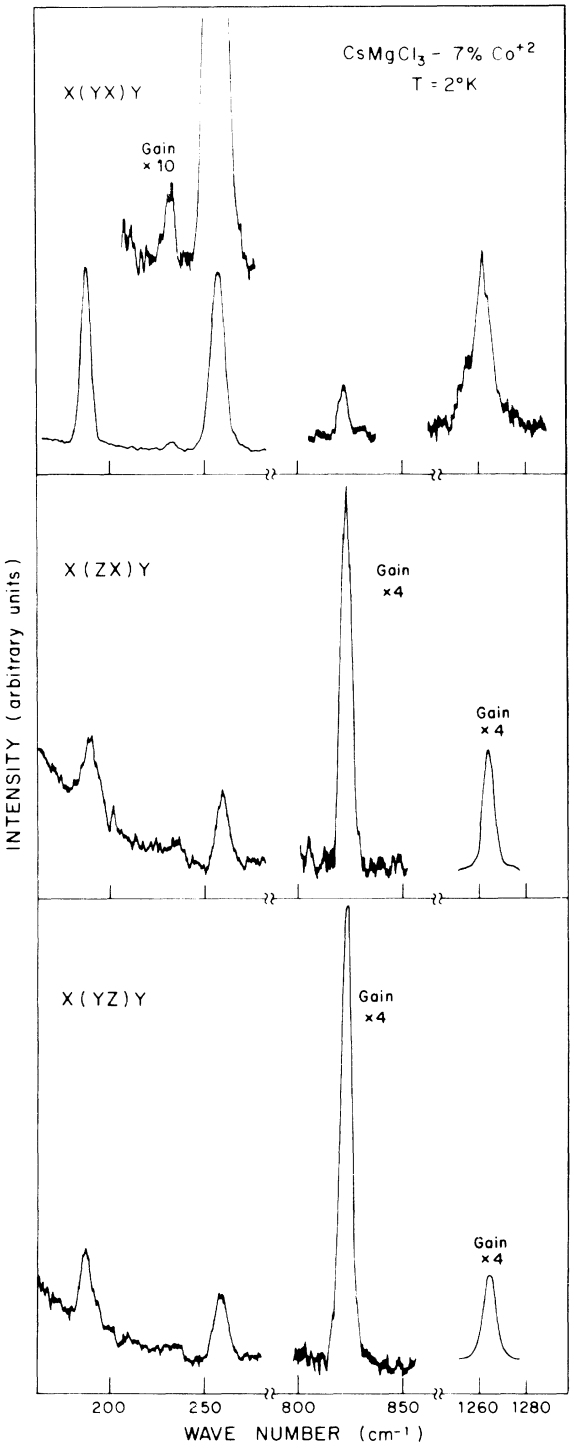

FIG. 1. Raman scattering of $CsMgCl_3$: 7-at.% Co^{2+} at 2 °K. No electronic lines are observed in zz polarization. The lines shifted by 189 and 258 cm^{-1} are due to phonon scattering.

this spectral region is weak and structureless and no resonance enhancement is expected. The observed intensities were corrected for both photomultiplier response and crystal absorption. Typical observed spectra are shown in Fig. 1. The lines shifted by 189 and 258 cm^{-1} are due to phonon scattering. They are observed in all other members of the $ABCl_3$ family (A is an alkaline ion, B is a transition-metal ion) which we have investigated. Also, they are the only lines observable at room temperature. The other three lines are due to scattering by the Co^{2+} ions. No electronic scattering was observed in zz polarization.

III. CRYSTAL-FIELD CALCULATION FOR $^4T_{1g}$ TERM

The ^4F term of a Co^{2+} ion subjected to a cubic octahedral crystalline field is split into three levels with energies $E(^4T_{1g}) = -6Dq$, $E(^4T_{2g}) = 2Dq$, and $E(^4A_{2g}) = 12Dq$. The wave functions are given by linear combinations of the form

$$|^4\Gamma_i\rangle = \sum_{M_L} a(\Gamma_i, M_L)\,|^4F, M_L\rangle. \tag{1}$$

The explicit expressions are given by Lines.[7] In this work we focus on the $^4T_{1g}$ term which is split further by the spin-orbit interaction and a residual crystal field due to the trigonal distortion from full cubic symmetry. The perturbing Hamiltonian is given by

$$\mathcal{H}' = V_{so} + V_{trig} = \lambda \vec{L}\cdot\vec{S} + B_1 L_z^2 + B_2 L_z^4. \tag{2}$$

The spin-orbit coupling constant deviates from the free-ion value because the $^4T_{1g}$ is perturbed by other $^4T_{1g}$ terms (outside ^4F). We shall take λ as a parameter to be fitted to the experimentally observed energy levels of $^4T_{1g}$. In first-order perturbation theory, the Hamiltonian given by Eq. (2) is customarily replaced by an effective Hamiltonian operating within $^4T_{1g}$:

$$\mathcal{H}'_{eff} = \lambda' \vec{\mathfrak{L}}\cdot\vec{S} - \Delta[\mathfrak{L}_z^2 - \tfrac{1}{3}\mathfrak{L}(\mathfrak{L}+1)]. \tag{3}$$

Here $\mathfrak{L}$ is a pseudo-angular-momentum of magnitude $\mathfrak{L} = 1$, $\lambda' = -\frac{3}{2}\lambda$, and $\Delta = \frac{3}{2}B_1 + \frac{63}{2}B_2$. An attempt was made previously[3] to fit $\mathcal{H}'_{eff}$ to the observed energy levels of Co^{2+} in $CdCl_2$ but it resulted in a significant inconsistency. In this study we have calculated the energies of the six Kramers doublets of $^4T_{1g}$ up to second order following a procedure developed by Pryce.[8] This approach is required because good wave functions are necessary for a reasonable calculation of the electronic Raman scattering (in addition to the above-mentioned difficulty). The energy eigenvalues of $^4T_{1g}$ up to second order are obtained by diagonalizing the 12×12 matrix whose elements are given by

$$V(M_{\mathcal{L}}M_S;\ M'_{\mathcal{L}}\ M'_S)=\langle {}^4T_{1g}M_{\mathcal{L}}M_S\,|\mathcal{H}'\,|\,{}^4T_{1g}M'_{\mathcal{L}}M'_S\rangle$$
$$-\frac{1}{E({}^4T_{2g})-E({}^4T_{1g})}\sum_{M''_{\mathcal{L}}M''_S}\langle {}^4T_{1g}M_{\mathcal{L}}M_S\,|\mathcal{H}'\,|\,{}^4T_{2g}M''_{\mathcal{L}}M''_S\rangle\langle {}^4T_{2g}M''_{\mathcal{L}}M''_S\,|\mathcal{H}'\,|\,{}^4T_{1g}M'_{\mathcal{L}}M'_S\rangle$$
$$-\frac{1}{E({}^4A_{2g})-E({}^4T_{1g})}\sum_{M''_S}\langle {}^4T_{1g}M_{\mathcal{L}}M_S\,|\mathcal{H}'\,|\,{}^4A_{2g}M''_S\rangle\langle {}^4A_{2g}M''_S\,|\mathcal{H}'\,|\,{}^4T_{1g}M'_{\mathcal{L}}M'_S\rangle, \quad (4)$$

where $M_{\mathcal{L}}=-1,0,1$ and $M_S=-\frac{3}{2},\ldots,\frac{3}{2}$.

The second-order part can be divided into three groups of terms in an obvious way: $V_{so}^{(2)}$, $V_{trig}^{(2)}$, and the mixed terms $V_{so\text{-}trig}^{(2)}$. Kanamori[9] has shown that the $V_{so}^{(2)}$ matrix is equivalent to the matrix of the following effective Hamiltonian calculated within the set of the ${}^4T_{1g}$ states:

$$V_{so}^{(2)}\rightarrow -\frac{15}{4}\frac{\lambda^2}{E({}^4T_{2g})-E({}^4T_{1g})}$$
$$\times[2(\mathcal{L}_\xi^2S_\xi^2+\mathcal{L}_\eta^2S_\eta^2+\mathcal{L}_\zeta^2S_\zeta^2)-(\vec{\mathcal{L}}\circ\vec{S})^2]. \quad (5)$$

$\mathcal{L}_\xi$, $\mathcal{L}_\eta$, $\mathcal{L}_\zeta$ are the components of $\vec{\mathcal{L}}$ along the [100] cubic axes.

Use of the full second-order Hamiltonian requires determination of three independent parameters: λ, B_1, and B_2. However, we have found that a very satisfactory fit to both energy levels and g factors of the ground state was obtained by restricting the number of parameters to two, λ and Δ, and by retaining $V_{so}^{(2)}$ only. Figure 2 shows the calculated energies of the six Kramers doublets of ${}^4T_{1g}$ as a function of $\Delta/|\lambda|$. The states are designated by the irreducible representations of the double group D_{3d}^* with an additional distinguishing label $(a, b, \ldots)$. The values of Δ corresponding to Co^{2+} in either $CdCl_2$ or $CsMgCl_3$ are denoted by arrows.

In order to obtain the values of λ and Δ for the crystals under study we have used the observed energy levels for the fitting procedure. Table I summarizes the results of the calculations, using both first- and second-order ($V_{so}^{(2)}$ only) perturbation theory as compared with the experimental data. The values of λ and Δ obtained by fitting the experimental data are listed in Table II. As a check on the adequacy of the obtained parameters we calculated $g_\parallel$ and $g_\perp$ of the (E_2, a) ground state. The results are compared in Table II with data obtained by ESR experiments.[10,11] Since the parameters obtained by second-order perturbation theory produce a better fit to both energy levels and g factors we have used them in the calculations of the Raman scattering intensities.

IV. ELECTRONIC RAMAN SCATTERING WITHIN ${}^4T_{1g}$ TERM

We now consider the inelastic scattering of light between the six Kramers doublets of the ${}^4T_{1g}$ term. As the experiments were done at low temperatures, the initial state of the Co^{2+} ion was the ground doublet $|g\rangle\equiv|E_2, a\rangle$, while the final state $|f\rangle$ was any one of the other five doublets (Fig. 2). The scattering intensity is determined by the polarizability tensor,[4] which is conveniently written as a sum of a symmetric and antisymmetric parts:

$$P_{\rho\sigma}(f,g,\nu)=P_{\rho\sigma}^{(S)}(f,g,\nu)+P_{\rho\sigma}^{(A)}(f,g,\nu)=\sum_n\frac{E_n}{E_n^2-(h\nu)^2}(\langle f|r_\sigma|n\rangle\langle n|r_\rho|g\rangle+\langle f|r_\rho|n\rangle\langle n|r_\sigma|g\rangle)$$
$$+\sum_n\frac{h\nu}{E_n^2-(h\nu)^2}(\langle f|r_\sigma|n\rangle\langle n|r_\rho|g\rangle-\langle f|r_\rho|n\rangle\langle n|r_\sigma|g\rangle). \quad (6)$$

Here E_n are the energies of the intermediate states $|n\rangle$ and $e\vec{r}$ is the ionic electric dipole operator; $\rho, \sigma = x, y, z$, where the first index corresponds to the polarization vector of the incident photon and the second to that of the scattered photon. ν is the frequency of the incident laser light, and it is implicitly assumed that $\nu=\nu_i\sim\nu_s$.

Now, for a divalent transition-metal ion located at a crystalline site having inversion symmetry, the first intermediate states that contribute to $P_{\rho\sigma}(f,g,\nu)$ belong to the $3d^{n-1}4p$ configuration. In the case of Co^{2+}, the $3d^64p$ configuration lies at about 100 000 cm^{-1}. From Eq. (6) it is noted that $P^{(A)}/P^{(S)}\sim h\nu/E_n$, which is roughly equal to 0.15 for laser light with $\nu\sim 15\,000$ cm^{-1}. Another important simplification arises from the fact that the intermediate states are far removed from the ${}^4T_{1g}$ ground term. According to Judd's closure approximation,[12] E_n is considered as being nearly constant for all the intermediate states. This assumption allows one[5] to express the polarizability tensor $P_{\rho\sigma}$ in terms of matrix elements of effec-

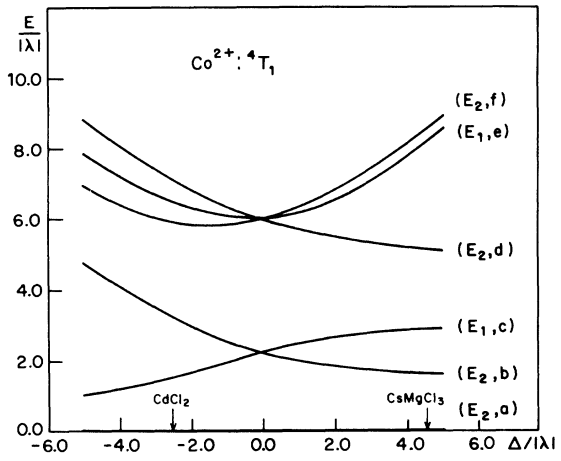

FIG. 2. Energy levels of the ground term ($^4T_{1g}$) of Co^{2+} calculated as a function of $\Delta/|\lambda|$. E_1 and E_2 denote the two irreducible representations of the double group D_{3d}^*.

tive tensor operators between the initial and final states of $^4T_{1g}$:

$$P_{\rho\sigma}(f,g,\nu)=\langle f\,|\sum_{k=0}^{2}\sum_{q=-k}^{k} c_{kq}(\rho,\sigma)\,\alpha_q^{(k)}\,|g\rangle\,. \qquad (7)$$

Explicit expressions are given, for instance, in Ref. 13. A typical equation is

$$P_{yx}(f,g,\nu)=\langle f\,|-\tfrac{1}{2}i(\alpha_2^{(2)}-\alpha_{-2}^{(2)}-\sqrt{2}\alpha_0^{(1)})|\,g\rangle\,.$$

We now employ the Wigner-Eckart theorem and note that all components $P_{\rho\sigma}(f,g,\nu)$ will depend on just two parameters: $\alpha_1'\equiv\langle {}^4T_{1g}\|\alpha^{(1)}\|{}^4T_{1g}\rangle$ and $\alpha_2'\equiv\langle {}^4T_{1g}\|\alpha^{(2)}\|{}^4T_{1g}\rangle$. $\alpha_0^{(0)}$ contributes to the Rayleigh scattering only. Of these two reduced matrix elements, α_1' determines the contribution of the antisymmetric part $P^{(A)}$ while α_2' determines that of the symmetric part $P^{(S)}$. The wave functions $|g\rangle$ and $|f\rangle$ describing the Kramers doublets of $^4T_{1g}$ can be written in the form of the following linear combinations:

$$|g\rangle=\sum_{M_{\mathcal{L}}=-1}^{1}\sum_{M_S=-3/2}^{3/2} b_g(M_{\mathcal{L}}M_S)\,|\mathcal{L},M_{\mathcal{L}}\rangle\,|S,M_S\rangle. \qquad (8)$$

The coefficients $b_g(M_{\mathcal{L}}M_S)$ are obtained in diagonalizing the V matrix of Eq. (4); they depend on the ratio $\Delta/|\lambda|$ only. Substituting for $|g\rangle$ and $|f\rangle$ in Eq. (7) we obtain

$$P_{\rho\sigma}(f,g,\nu)=\sum_{M_{\mathcal{L}}M_{\mathcal{L}}',M_SM_S'} b_f^*(M_{\mathcal{L}}'M_S')\,b_g(M_{\mathcal{L}}M_S)\delta_{M_SM_S'}\langle\mathcal{L},M_{\mathcal{L}}'|\sum_{kq}c_{kq}(\rho,\sigma)\,\alpha_q^{(k)}\,|\mathcal{L},M_{\mathcal{L}}\rangle$$

$$\equiv\sum_{M_{\mathcal{L}}M_{\mathcal{L}}',M_S} b_f^*(M_{\mathcal{L}}'M_S)\,b_g(M_{\mathcal{L}}M_S)\,\alpha_{\rho\sigma}(M_{\mathcal{L}}',M_{\mathcal{L}}). \qquad (9)$$

The matrices $\alpha_{\rho\sigma}(M_{\mathcal{L}}',M_{\mathcal{L}})$ are defined by Eq. (9). Their elements are dependent on α_1' and α_2'. In the Appendix we give their explicit form for $^4T_{1g}$ of Co^{2+}.

We have thus shown that $P_{\rho\sigma}(f,g,\nu)$ depends on the ratio $\Delta/|\lambda|$ through the coefficients b_f and b_g and on the reduced matrix elements α_1' and α_2' through the matrices $\alpha_{\rho\sigma}$. We note that only the relative intensities of lines for a given scattering configuration (i.e., given ρ and σ) are usually determined experimentally. Thus, only the ratio α_1'/α_2' is determined. The transition probability for scattering between levels g and f can then be computed as a function of two ratios: $\Delta/|\lambda|$ and α_1'/α_2'. We should bear in mind that in so doing, the separate contributions of each independent transition between the Kramers components of g and f are summed up:

$$W_{\rho\sigma}(f,g,\Delta/|\lambda|,\alpha_1'/\alpha_2')\propto\sum_{i,j}|P_{\rho\sigma}(f_i,g_j,\nu)|^2. \qquad (10)$$

TABLE I. Observed and calculated energy levels for the $^4T_{1g}$ term of Co^{2+} in $CdCl_2$ and $CsMgCl_3$.

State	Observed energy (cm^{-1})	Calculated energies: First order	Second order
	(a) $CsMgCl_3:Co^{2+}$		
E_2,a	0	0	0
E_2,b	235 ± 3	263	241
E_1,c	...	457	446
E_2,d	823 ± 2	819	823
E_1,e	1265 ± 3	1266	1266
E_2,f	...	1327	1371
	(b) $CdCl_2:Co^{2+}$ [a]		
E_2,a	0	0	0
E_1,c	...	236	211
E_2,b	500	487	491
E_2,f	923	899	908
E_1,e	953	981	973
E_2,d	...	1083	1108

[a] Data of Ref. 3.

TABLE II. Spin-orbit and trigonal-crystal-field parameters and ground-state g factors.

	$CsMgCl_3:Co^{2+}$	$CdCl_2:Co^{2+}$
First-order perturbation		
λ (cm^{-1})	−159	−152
Δ (cm^{-1})	680	−378
$g_\parallel$	6.90	2.90
$g_\perp$	2.50	4.94
Second-order perturbation		
λ (cm^{-1})	−166	−159
Δ (cm^{-1})	727	−405
$g_\parallel$	7.03	2.85
$g_\perp$	2.68	4.96
Observed g factors		
$g_\parallel$	7.32[a]	2.97
$g_\perp$		4.95[b]

[a] Data of Ref. 11. [b] Data of Ref. 10.

i and j denote the individual Kramers components of f and g, respectively. We shall refer to the expression on the right-hand side of Eq. (10) as the spectral intensity of the (f,g) scattering in $\rho\sigma$ polarization configuration.

The calculated spectral intensities as a function of $\Delta/|\lambda|$ of the five electronic Raman transitions are shown in Figs. 3 and 4. Figure 3 shows the

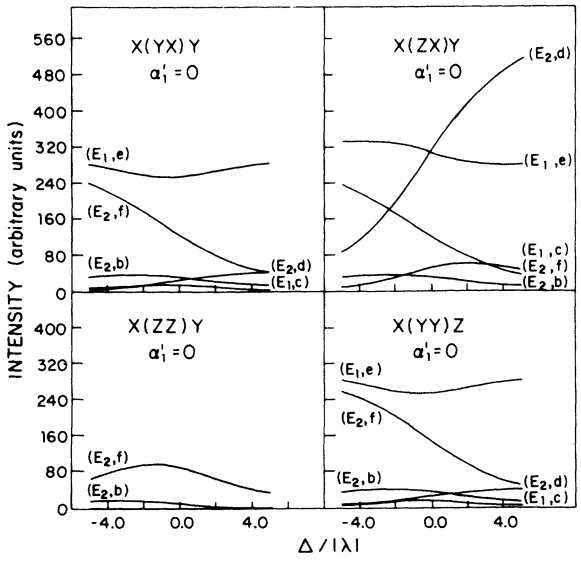

FIG. 3. Electronic Raman spectral intensity for scattering between the ground level (E_2,a) and the five excited levels of $^4T_{1g}$ as a function of $\Delta/|\lambda|$. The antisymmetric scattering is assumed to vanish.

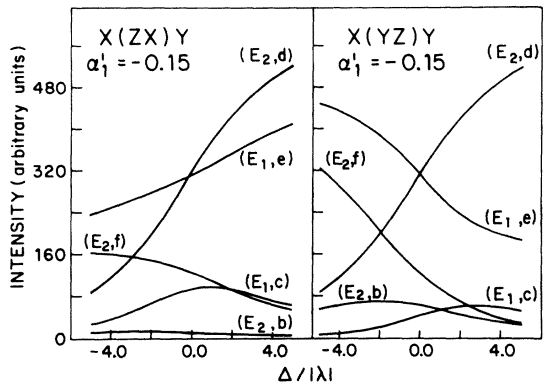

FIG. 4. Effect of nonvanishing antisymmetric scattering on the spectral intensities in zx and yz polarization.

results for the case $\alpha_1'=0$, i.e., only the symmetric scattering. Since the effect of the antisymmetric part ($\alpha_1'\neq 0$) could be determined experimentally by observing the asymmetry between zx and yz scattering configurations, we show in Fig. 4 only these two polarizations, calculated with $\alpha_1'/\alpha_2' = -0.15$. (For $\alpha_1'/\alpha_2' = +0.15$ the zx and yz spectral intensities of each transition are merely interchanged with respect to the case with $\alpha_1'/\alpha_2' = -0.15$.) In comparing the zx and yz spectral intensities it is worthwhile noting that the $(E_2, a) \rightarrow (E_2, d)$ transition has equal intensities for both configurations. This behavior is due to the fact that this transition is the only one that is independent of α_1'.

We now apply the results of these calculations to the experimental data of Sec. II. For $CsMgCl_3:Co^{2+}$ we have a complete polarization analysis of the experimental transitions. The $\Delta/|\lambda|$ ratio was determined by fitting the energies of the observed levels. The α_1'/α_2' ratio was determined by a χ^2 fit of the scattering intensities of the (E_2,d) and

TABLE III. Observed and calculated (parentheses) spectral intensities of electronic Raman lines for $CsMgCl_3:Co^{2+}$. (All lines in each polarization are normalized with respect to the intensity of the 1265-cm^{-1} line.)

Pol.	E_2,b 235 cm^{-1}	E_1,c 446	E_2,d 823	E_1,e 1265	E_2,f 1371
$x(yx)y$	...	...	0.18 ± 0.03	1.0	...
	(0.07)	(0.02)	(0.14)	(1.0)	(0.16)
$x(yz)y$	...	...	2.28 ± 0.1	1.0	...
	(0.01)	(0.23)	(2.28)	(1.0)	(0.17)
$x(zx)y$	...	...	1.55 ± 0.1	1.0	...
	(0.02)	(0.16)	(1.42)	(1.0)	(0.14)

(E_1, e) lines in zx and yz polarizations. We thus obtain

$$\alpha_1'/\alpha_2' = -0.09 \pm 0.05 \quad (CsMgCl_3:Co^{2+}). \qquad (11)$$

Using this value we calculated the scattering spectral intensities for all lines in all polarizations and compared them with the experimental results (Table III). In this table all intensities are normalized with respect to the (E_1, e) line intensity. The agreement between experiment and theory is quite adequate: (a) The intensities of all lines are predicted to be weakest for zz polarization. No scattering is observed experimentally. (b) The strongest line in yx polarization corresponds to the (E_1, e) doublet, while in yz and zx polarizations the strongest lines correspond to the (E_2, d) and (E_1, e) doublets.

In the case of $CdCl_2:Co^{2+}$ we lack a complete polarization analysis. As mentioned in Sec. II, the configuration used in Ref. 3 is compatible with a yx and zx combination. From Fig. 3 we note that for $\Delta/|\lambda| = -2.5$ two strong transitions are expected in yx polarization: (E_1, e) and (E_2, f). In zx polarization these two lines are again expected to be strong. This general behavior is in qualitative agreement with experiment.

V. SUMMARY

The electronic Raman scattering between the crystal-field states of the lowest $^4T_{1g}$ term of Co^{2+} has been examined both experimentally and theoretically. We have shown that the energy levels are well accounted for when second-order perturbation theory is used. The resulting wave functions have been used to calculate the Raman intensities as a function of $\Delta/|\lambda|$ and for two given values of α_1'/α_2'. Good agreement is obtained between experiment and calculation for both $CsMgCl_3:Co^{2+}$ and $CdCl_2:Co^{2+}$, for which $\Delta/|\lambda| > 0$ and $\Delta/|\lambda| < 0$, respectively. The facts that the closure approximation works well and that the antisymmetric part is small for Co^{2+} are explained by noting that the intermediate configuration involved lies at about 100 000 cm^{-1}. It is interesting to contrast this case with rare-earth ions like Ce^{3+},[4] Nd^{3+},[13] and Dy^{3+}.[14] For these ions large antisymmetric scattering is observed, and the closure approximation on the intermediate states is not as good as in Co^{2+}. This is due to the fact that the $4f^n$ and $4f^{n-1}\,5d$ configurations are closer in energy than $3d^n$ and $3d^{n-1}\,4p$.

Finally, a good knowledge of the single-ion eigenfunctions is a prerequisite for a detailed study of the elementary excitations in the isomorphic concentrated crystals. Such a study in $CoCl_2$ is the subject of a forthcoming publication.

APPENDIX

The following are explicit expressions of the matrices $\alpha_{\rho\sigma}(M_{\mathcal{L}}', M_{\mathcal{L}})$ defined by Eq. (9). α_1' and α_2' are the reduced matrix elements of the $\alpha^{(1)}$ and $\alpha^{(2)}$ tensors within the $^4T_{1g}$ term.

α_{yx}:

$M_{\mathcal{L}}$ \ $M_{\mathcal{L}}'$	-1	0	1
-1	$\frac{3}{8}\sqrt{\frac{2}{21}}\,\alpha_1'$	$-\frac{5}{12}\sqrt{\frac{1}{70}}\,\alpha_2'$	$\frac{1}{6}\sqrt{\frac{1}{70}}\,\alpha_2'$
0	$\frac{5}{12}\sqrt{\frac{1}{70}}\,\alpha_2'$	0	$\frac{5}{12}\sqrt{\frac{1}{70}}\,\alpha_2'$
1	$-\frac{1}{6}\sqrt{\frac{1}{70}}\,\alpha_2'$	$-\frac{5}{12}\sqrt{\frac{1}{70}}\,\alpha_2'$	$-\frac{3}{8}\sqrt{\frac{2}{21}}\,\alpha_1'$

α_{yy}:

$-\frac{1}{12}\sqrt{\frac{1}{70}}\,\alpha_2'$	$\frac{5}{12}\sqrt{\frac{1}{70}}\,\alpha_2'$	$\frac{1}{6}\sqrt{\frac{1}{70}}\,\alpha_2'$
$\frac{5}{12}\sqrt{\frac{1}{70}}\,\alpha_2'$	$\frac{1}{6}\sqrt{\frac{1}{70}}\,\alpha_2'$	$-\frac{5}{12}\sqrt{\frac{1}{70}}\,\alpha_2'$
$\frac{1}{6}\sqrt{\frac{1}{70}}\,\alpha_2'$	$-\frac{5}{12}\sqrt{\frac{1}{70}}\,\alpha_2'$	$-\frac{1}{12}\sqrt{\frac{1}{70}}\,\alpha_2'$

α_{zz}:

$-\frac{1}{6}\sqrt{\frac{1}{70}}\,\alpha_2'$	0	0
0	$\frac{1}{3}\sqrt{\frac{1}{70}}\,\alpha_2'$	0
0	0	$-\frac{1}{6}\sqrt{\frac{1}{70}}\,\alpha_2'$

α_{zx}:

0	$\frac{3}{8}\sqrt{\frac{1}{21}}\,\alpha_1' + \frac{7}{24}\sqrt{\frac{1}{35}}\,\alpha_2'$	$\frac{5}{12}\sqrt{\frac{1}{35}}\,\alpha_2'$
$-\frac{3}{8}\sqrt{\frac{1}{21}}\,\alpha_1' + \frac{7}{24}\sqrt{\frac{1}{35}}\,\alpha_2'$	0	$\frac{3}{8}\sqrt{\frac{1}{21}}\,\alpha_1' - \frac{7}{24}\sqrt{\frac{1}{35}}\,\alpha_2'$
$\frac{5}{12}\sqrt{\frac{1}{35}}\,\alpha_2'$	$-\frac{3}{8}\sqrt{\frac{1}{21}}\,\alpha_1' - \frac{7}{24}\sqrt{\frac{1}{35}}\,\alpha_2'$	0

α_{yz}:

$$\begin{pmatrix} 0 & -\frac{3}{8}\sqrt{\frac{1}{21}}\alpha_1' + \frac{7}{24}\sqrt{\frac{1}{35}}\alpha_2' & -\frac{5}{12}\sqrt{\frac{1}{35}}\alpha_2' \\ -\frac{3}{8}\sqrt{\frac{1}{21}}\alpha_1' - \frac{7}{24}\sqrt{\frac{1}{35}}\alpha_2' & 0 & -\frac{3}{8}\sqrt{\frac{1}{21}}\alpha_1' - \frac{7}{24}\sqrt{\frac{1}{35}}\alpha_2' \\ \frac{5}{12}\sqrt{\frac{1}{35}}\alpha_2' & -\frac{3}{8}\sqrt{\frac{1}{21}}\alpha_1' + \frac{7}{24}\sqrt{\frac{1}{35}}\alpha_2' & 0 \end{pmatrix}$$

---

*On leave of absence from the Department of Physics, Technion, Haifa, Israel.

[1]A. Ishikawa and T. Moriya, J. Phys. Soc. Jap. 30, 117 (1971); P. A. Fleury and R. Loudon, Phys. Rev. 166, 514 (1968).

[2]B. F. Gächter and J. A. Koningstein, Chem. Phys. Lett. 23, 28 (1973) (Fe^{2+}); J. A. Koningstein, P. A. Grunberg, J. T. Hoff, and J. M. Preudhomme, J. Chem. Phys. 56, 354 (1972) (Co^{2+}).

[3]D. L. Lockwood and J. M. Christie, Chem. Phys. Lett. 9, 559 (1971).

[4]A. Kiel, T. Damen, S. P. S. Porto, S. Singh, and F. Varsanyi, Phys. Rev. 178, 1518 (1969).

[5]J. D. Axe, Phys. Rev. 136, A42 (1964).

[6]A. Sorgen, E. Cohen, and J. Makovsky, Phys. Rev. B10, 4643 (1974).

[7]M. E. Lines, Phys. Rev. 131, 546 (1963).

[8]M. H. L. Pryce, Proc. Phys. Soc. Lond. 63, 25 (1950).

[9]J. Kanamori, Prog. Theor. Phys. 17, 177 (1957).

[10]K. Morigaki, J. Phys. Soc. Jpn. 16, 1639 (1961).

[11]N. Achiwa, J. Phys. Soc. Jpn. 27, 561 (1969).

[12]B. R. Judd, Phys. Rev. 127, 750 (1962).

[13]E. Finkman, E. Cohen, and L. G. Van Uitert, Phys. Rev. B 7, 2899 (1973).

[14]R. L. Wadsac, J. L. Lewis, B. E. Argyle, and R. K. Chang, Phys. Rev. B 3, 4342 (1971).